Human Molecular Genetics, 2013, Vol. 22, No. 14 ***2775–2784***
doi:10.1093/hmg/ddt125
Advance Access published on March 19, 2013

Triplication of *DYRK1A* causes retinal structural and functional alterations in Down syndrome

Ariadna Laguna[1,2,†,‡], María-José Barallobre[1,†], Miguel-Ángel Marchena[3,†], Catarina Mateus[4], Erika Ramírez[2], Carmen Martínez-Cue[5], Jean M. Delabar[6], Miguel Castelo-Branco[4], Pedro de la Villa[3] and Maria L. Arbonés[1,*]

[1]Department of Developmental Biology, Institut de Biologia Molecular de Barcelona (IBMB-CSIC), and Centro de Investigación Biomédica en Red de Enfermedades Raras (CIBERER), Barcelona 08028, Spain, [2]Centre de Regulació Genòmica (UPF), Barcelona 08003, Spain, [3]Department of Physiology, School of Medicine, Universidad de Alcalá, Alcalá de Henares 28871, Spain, [4]Visual Neuroscience Laboratory, IBILI, Faculty of Medicine, University of Coimbra, Coimbra 3000-548, Portugal, [5]Department of Physiology and Pharmacology, Faculty of Medicine, University of Cantabria, Santander 39011, Spain and [6]Unité de Biologie Fonctionnelle et Adaptative (BFA), EAC CNRS 4413, Université Paris Diderot, Paris 75205, France

Received February 7, 2013; Revised and Accepted March 13, 2013

Down syndrome (DS) results from the triplication of approximately 300 human chromosome 21 (Hsa21) genes and affects almost all body organs. Children with DS have defects in visual processing that may have a negative impact on their daily life and cognitive development. However, there is little known about the genes and pathogenesis underlying these defects. Here, we show morphometric *in vivo* data indicating that the neural retina is thicker in DS individuals than in the normal population. A similar thickening specifically affecting the inner part of the retina was also observed in a trisomic model of DS, the Ts65Dn mouse. Increased retinal size and cellularity in this model correlated with abnormal retinal function and resulted from an impaired caspase-9-mediated apoptosis during development. Moreover, we show that mice bearing only one additional copy of *Dyrk1a* have the same retinal phenotype as Ts65Dn mice and normalization of *Dyrk1a* gene copy number in Ts65Dn mice completely rescues both, morphological and functional phenotypes. Thus, triplication of *Dyrk1a* is necessary and sufficient to cause the retinal phenotype described in the trisomic model. Our data demonstrate for the first time the implication of DYRK1A overexpression in a developmental alteration of the central nervous system associated with DS, thereby providing insights into the aetiology of neurosensorial dysfunction in a complex disease.

INTRODUCTION

Down syndrome (DS), occurring 1 in 700 live births approximately, is a complex developmental disorder caused by trisomy of human chromosome 21 (Hsa21). Although the clinical manifestations in DS are variable, all cases exhibit intellectual disabilities (1,2). Ophthalmic disorders are common clinical manifestations in children with DS (3,4). Nonetheless, visual acuity and contrast sensitivity in these children are reduced (5) even in the absence of such disorders (6–8), indicating abnormal function of the neural visual pathway in this population. In fact, defects in retino-cortical visual processing have been identified in DS infants (9,10) and adults (10) by the alterations observed in cortical visual evoked potential (VEP). Evaluation of the dendritic branching in post-mortem tissue suggested that abnormalities in the formation of the visual cortex circuitry might contribute to these alterations (11). However, and despite the negative impact that visual defects may have on normal daily life and cognitive

*To whom correspondence should be addressed at: IBMB-CSIC, Barcelona Science Parc, c/ Baldiri i Reixac 4-8, 08028 Barcelona, Spain. Tel: +34 934034668; Fax: +34 934034979; Email: marbmc@ibmb.csic.es
†These authors contributed equally to this work.
‡Present address: Ludwig Institute for Cancer Research, Karolinska Institutet, Stockholm, Sweden.

development (12), the pathological mechanisms underlying abnormal visual processing in trisomy 21 have not been further investigated, probably because of the scarcity of post-mortem tissue and the difficulty in using available non-invasive techniques in DS patients.

The detection, initial processing and transmission of visual inputs to the brain depend on the correct assembly of six principal types of neurons into a functional layered structure, the retina (13). The neural retina is part of the central nervous system (CNS) and, therefore, its development is regulated by the same fundamental cellular and molecular mechanisms that regulate growth and generate cell diversity in the brain (14). The developing retina expresses several Hsa21 genes that have known functions in CNS development (15–18) and are strong candidates to participate in the neurological phenotype and cognitive deficits associated with DS (19). Thus, the overexpression of one or several of such genes in the retina could alter its functional architecture, contributing to the visual defects in DS. In this work, we show *in vivo* data indicating developmental alterations in the neural retina of DS individuals. To get some insights into the aetiology of these alterations, we have used a murine model of human trisomy 21 (the Ts65Dn mouse), which displays many aspects of the DS phenotype (20) and in particular, VEP abnormalities that are similar to those reported in DS (21). Our results show that developmental apoptosis in the retina of Ts65Dn mice is significantly impaired, leading to an increased size and cellularity, as well as an abnormal function of the adult retina. Importantly, we demonstrate that triplication of *DYRK1A* (*dual-specificity tyrosine-(Y)-phosphorylation regulated kinase 1A*) gene, formerly known as *MNB* (22), is necessary and sufficient to produce the retinal phenotype in this model.

RESULTS

DS subjects present a thickening of the neural retina

Trisomy 21 changes the normal size and shape of the brain (23). To identify any possible structural alteration of the retina that may contribute to the neural visual deficits observed in DS, we assessed the detailed structure of the retina in three patients with DS (five retinas) using spectral-domain optical coherence tomography [SD-OCT (24)]. Optical biopsies obtained at different regions of the retina did not reveal any gross alteration in its general organization (Fig. 1A). However, the comparison of the morphometric data obtained from the retinas of DS patients with those obtained from an age-matched database of control subjects (16 retinas) revealed that DS subjects had a thicker neural retina than the controls, which was particularly significant in the central foveomacular region (Fig. 1B–D). This is a surprising finding considering that hypoplasia of the brain

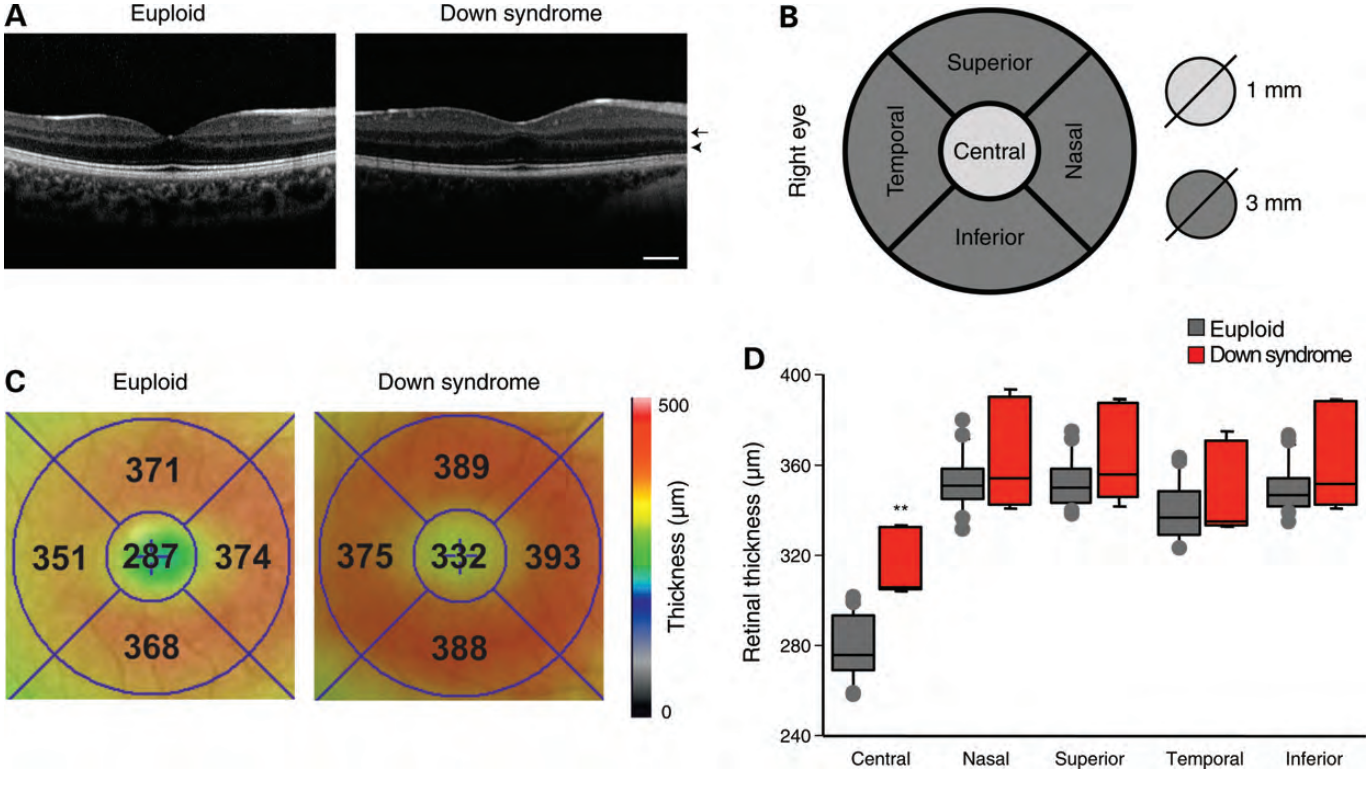

Figure 1. Microstructural alterations of the central retina in DS. (**A**) Representative optical biopsy of the central foveomacular region from the retina of a control (euploid) and DS subject obtained using SD-OCT. The lower hyperreflective layer corresponds to the pigment epithelium and the upper layer to the GC retinal nerve fibre layer. Note that the inner nuclear layer (the first dark stripe from the top; see the arrow) is thicker in the DS subject, whereas the outer nuclear layer (the second dark stripe from the top; see the arrowhead) does not seem to be altered. (**B**) Geometric layout of the retinal regions sampled: foveomacular (central), nasal, temporal, inferior and superior. (**C**) Representative colour-coded thickness map of one control and one DS retina in which the numbers correspond to the thickness (in microns) of each retinal region. (**D**) Box plots showing the average thickness and distribution of the five retinal regions analysed in control (16 eyes) and DS subjects ($n = 5$). Differences are statistically different only in the central region, $^{**}P < 0.001$.

and cerebellum is a more common characteristic of the syndrome (23). Nevertheless, it indicates that the functionality of the retina may be altered in DS.

The Ts65Dn mouse model presents hyperplasia of the inner part of the retina as a result of less developmental apoptosis

To define better the retinal phenotype observed in DS subjects and investigate its aetiology, we performed a detailed morphometric analysis of the central retina in young adult trisomic Ts65Dn mice and their euploid control littermates. As in humans, the retina of trisomic mice had a normal layered organization but was slightly thicker than in the control group (Fig. 2A). Although the thickness of the photoreceptor (PR) layer (outer nuclear layer—ONL) was similar in mutant and control retinas, the thickness of the inner nuclear layer (INL) was greater in Ts65Dn mice (Fig. 2A and Supplementary Material, Table S1). Interestingly, a thickening of the INL, but not of the ONL, was appreciated in the DS subjects examined (Fig. 1B). The inner plexiform layer (IPL), where INL cells synapse with ganglion cells (GCs), was also wider in the trisomic mice and there were more cells in the GC layer (Fig. 2A and Supplementary Material, Table S1). A similar anatomical defect specifically affecting the size and cellularity of the inner retina was previously observed in another DS model, the hYACtg152f7 mouse (25), which carries a small segment of the Down syndrome critical region (*DSCR*) containing four genes (*PIGP*, *TTC3*, *DSCR3* and *DYRK1A*) of the approximately 100 trisomic genes in the Ts65Dn model (26). *In vivo* rescue experiments identified *DYRK1A* as the gene responsible for the phenotype (16). As the increase in *Dyrk1a* gene copy number in Ts65Dn mice results in a 50% increase in the amount of Dyrk1a protein in the retina (Supplementary Material, Fig. S1), *Dyrk1a* could be the trisomic gene provoking hyperplasia of the inner retina in the Ts65Dn model.

Mitochondrial-dependent cell death (27) is fundamental in adjusting the absolute number and proportion of retinal cells during development (28,29), a process that is negatively regulated by DYRK1A-mediated phosphorylation of caspase-9 (Casp9) (16). To assess whether the abnormal size and cellularity in the retina of Ts65Dn mice are a result of reduced developmental cell death, as occurs in the hYACtg152f7 model (16), we counted the number of retinal cells expressing active Casp9 and caspase-3 (Casp3) in postnatal day (P)0 Ts65Dn and control mice. The number of both active Casp3- and Casp9-immunolabelled cells decreased significantly in the

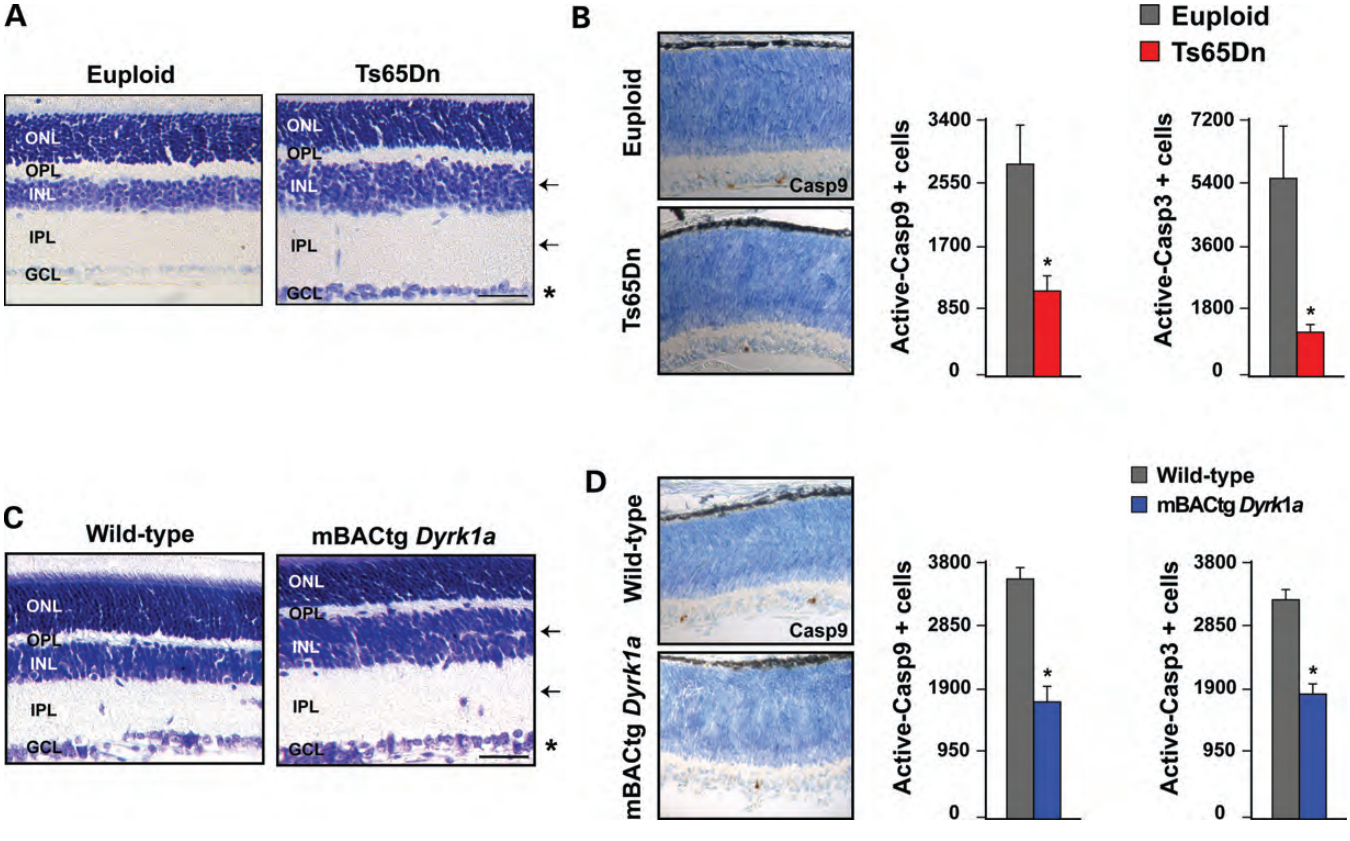

Figure 2. Ts65Dn and mBACtg*Dyrk1a* mice present greater cellularity in the inner part of the retina as a result of less developmental apoptosis. Representative eye sections obtained at the level of the central retina from adult Ts65Dn (**A**) and mBACtg*Dyrk1a* (**C**) mice, and from control littermates, euploid and wild-type, respectively, all stained with cresyl violet acetate. Note that the thickness of the INL and IPL indicated by arrows, but not that of the ONL and OPL (outer plexiform layer), is greater in the mutant retinas than in the controls. The cellularity of the GCL (ganglion cell layer) is also greater in the mutants (asterisks). All quantifications are summarized in Supplementary Material, Tables S1 and S2. Scale bars correspond to 40 μm. Representative images of the retina showing cells with active Casp9 (in brown) and histograms showing the average numbers of cells with active Casp9 and active Casp3 in retinas from P0 Ts65Dn (**B**) and mBACtg*Dyrk1a* (**D**) mice, and their respective controls: $n = 5$ (euploid); $n = 4$ (Ts65Dn); $n = 4$ (wild-type); $n = 5$ (mBACtg*Dyrk1a*). $^*P < 0.05$.

mutant retinas (Fig. 2B), suggesting that inhibition of Casp9-mediated cell death may be the molecular cause underlying the increase in retinal size in Ts65Dn mice.

mBACtg*Dyrk1a* mice present similar morphological retinal alterations as Ts65Dn mice

The above experiments indicated that the increase in *Dyrk1a* gene copy number could be the cause of the retinal size alterations in the trisomic Ts65Dn mouse model. To assess this possibility, we repeated the same retinal quantifications in a transgenic model that carries three copies of the mouse *Dyrk1a* gene, the *mBACtgDyrk1a* model (30). As in the trisomic model, *mBACtgDyrk1a* mice show a 50% increase in the amount of Dyrk1a protein in the retina (Supplementary Material, Fig. S1). The thickness of the retina INL and IPL and the cellularity of the GC layer were increased in adult mBACtg-*Dyrk1a* mice to a similar extent than in the Ts65Dn model (Fig. 2A and C). Moreover, the quantification of active Casp3- and Casp9-immunolabelled cells in the retina of P0 mBACtg*Dyrk1a* and control mice (Fig. 2D) indicated that, as in the Ts65Dn model, the increase in retinal size in the transgenic model results from a decrease in Casp9-mediated apoptosis. This result strongly suggests that triplication of *Dyrk1a* causes the retinal size alterations observed in Ts65Dn mice.

Reverting *Dyrk1a* gene copy number normalizes retinal developmental apoptosis in Ts65Dn mice

To prove that *Dyrk1a* is the gene involved in the phenotype described in the trisomic model, we quantified the developmental cell death in the retina of the progeny born from crosses between Ts65Dn mice and $Dyrk1a^{+/-}$ mice (31). In the retina of Ts65Dn (Ts$Dyrk1a^{+++}$) mice, the number of active Casp9 cells was again significantly reduced (Fig. 3B). In contrast, normal levels of cell death were evident in the retinas of Ts65Dn mice with a diploid complement of *Dyrk1a* (Ts$Dyrk1a^{++-}$ mice) and thus, with normal Dyrk1a protein levels (Fig. 3A and B). Consistent with published data (16), lowering *Dyrk1a* gene dosage to one copy in euploid mice ($Dyrk1a^{+/-}$ mice) dramatically increased Casp9-mediated cell death (Fig. 3B). These results show that Casp9-mediated cell death in the trisomic retina depends on *Dyrk1a* gene copy number. In addition, they suggest that the effect of Dyrk1a overexpression on retina growth is independent of the mouse genetic background. To provide evidence of this, we again assessed the morphology of the outer and inner retinal layers in such mice 30 days later, after the main waves of programmed cell death in the retina have occurred (32–34), and the five layers of the retina are well defined (Fig. 3C). The INL and IPL were thicker in trisomic Ts$Dyrk1a^{+++}$ mice, whereas the thickness of the outer retinal layers remained normal (Fig. 3C and D), as in older trisomic mice (Fig. 2A). In accordance with the cell death data, normalization of *Dyrk1a* gene copy number in Ts65Dn mice (Ts$Dyrk1a^{++-}$ mice) decreased the thickness of the inner retina to normal values without affecting the width of the outer retina (Fig. 3C and D). The specific thinning of the internal layers in $Dyrk1a^{+/-}$ mice is consistent with the inhibitory effect of DYRK1A on retinal cell death during development (16). These data indicate that the inhibition of physiological apoptosis due to the extra copy of *Dyrk1a* alters the cellularity in the retina of Ts65Dn mice.

Ts65Dn and mBACtg*Dyrk1a* mice present an abnormal retinal function

Transmission of light stimuli from PR cells to GCs—the cells that send the information to the brain—can be evaluated in the whole animal by electroretinogram (ERG) recordings. The functionality of the retina in the Ts65Dn model has been previously evaluated, but the mean peaks measured in the ERG responses obtained in trisomic mice were not significantly different from those obtained in euploid animals (21). Several mutant mice that have an altered cellularity in the internal layers of the retina, like the hYACtg152f7 DS mouse model (16), the $Dyrk1a^{+/-}$ mouse (16) and the *Bhlhb4* (35) and *Math5* (36) knockout mice, present defects in the electrical currents generated in these layers. In view of these observations and the defects in retinal size and cellularity reported above (Fig. 2 and Supplementary Material, Table S1), we dissected out the electrophysiological waves originated from the different retina components in the Ts65Dn mice as we did before in the hYACtg152f7 and $Dyrk1a^{+/-}$ models (16). For this, we obtained ERGs from adult trisomic animals and euploid littermates under scotopic and photopic conditions in order to evaluate the rod and cone pathways, respectively. Scotopic and photopic b-wave amplitudes were larger in the Ts65Dn mice than in their euploid controls (Fig. 4A, B and D), indicating that the activity of cells post-synaptic to the rod and cone PRs was enhanced in the trisomic state. In contrast, the amplitudes of scotopic a-waves were normal (Fig. 4B), reflecting the functionality of rod and cone PRs (37). The flicker responses generated under photopic stimulation (Fig. 4E) also indicate that cone PR function is not significantly altered in the trisomic model. Maximum oscillatory potentials (OPs) were stronger in Ts65Dn mice (Fig. 4C), reflecting abnormal extracellular electrical currents generated by negative feedback pathways between second- and third-order neurons in the IPL. Together, these results, summarized in Figure 4F, indicate that retinal activity in adult Ts65Dn mice is enhanced mainly due to altered light transmission through inner retina cells, and the specificity of this dysfunction points to the defect in cellularity as the underlying cause. To provide further evidence of this, we repeated the functional analysis in adult mBACtg*Dyrk1a* and control littermate mice. The analysis showed that the responses to light stimuli that are affected in the Ts65Dn mice (Fig. 4) are identically affected in the mBACtg*Dyrk1a* model (see ERG responses in Supplementary Material, Fig. S2).

Together, these results show that Ts65Dn mice have an abnormal retinal activity, which likely results from the increased cellularity of the inner retina.

Reverting *Dyrk1a* gene copy number in Ts65Dn mice normalizes retinal activity

Given the data obtained, the enhanced retinal responses to light stimuli in Ts65Dn mice appear to be caused by Dyrk1a

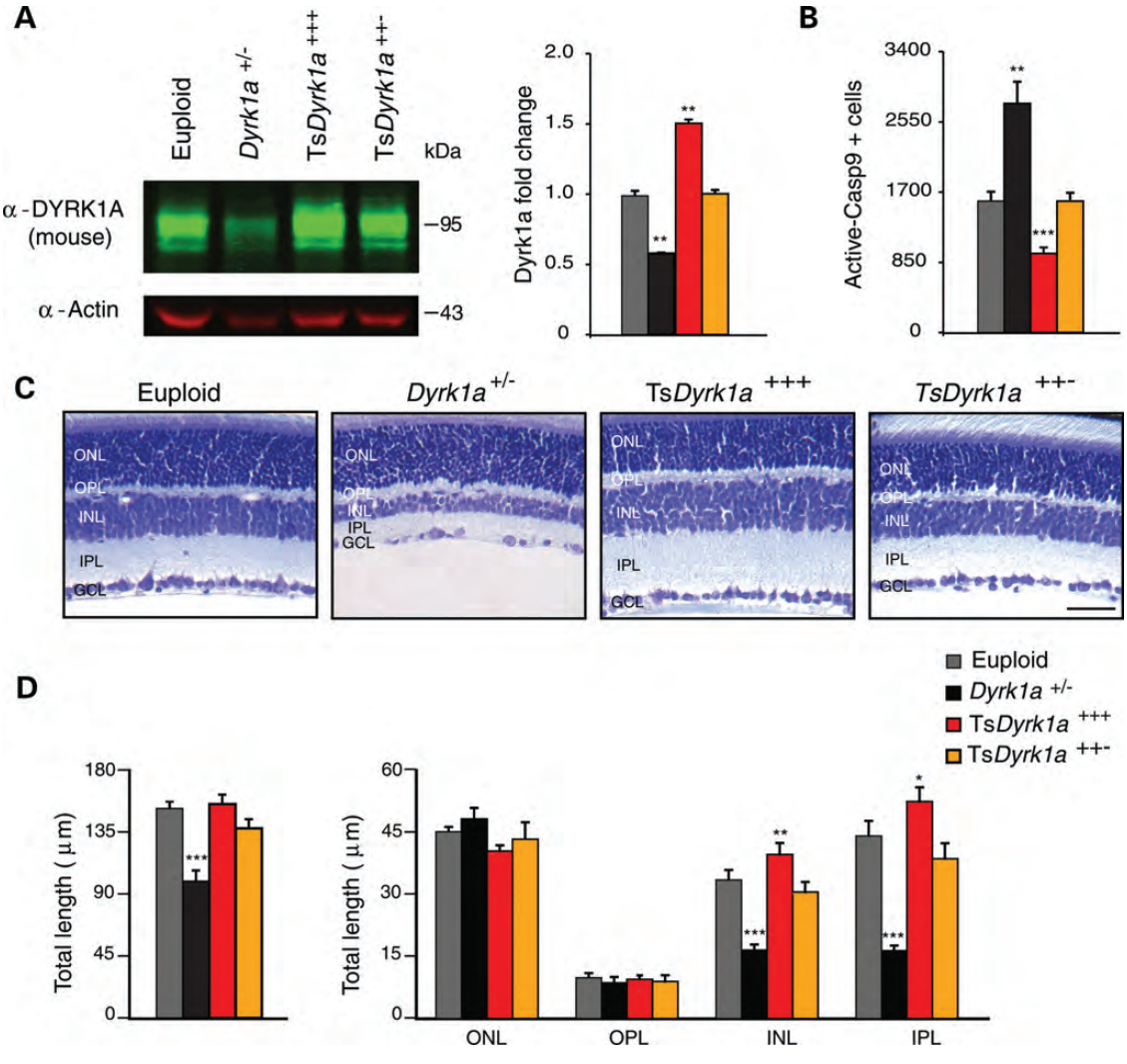

Figure 3. Ts65Dn retinas with two functional copies of *Dyrk1a* are normal in size and display normal developmental cell death. (**A**) Western blot of Dyrk1a expression in total retinal lysates prepared from control $Dyrk1a^{+/+}$ (euploid), $Dyrk1a^{+/-}$ (one copy of *Dyrk1a*), Ts65Dn (Ts$Dyrk1a^{+++}$; three copies of *Dyrk1a*) and Ts65Dn with two copies of *Dyrk1a* (Ts$Dyrk1a^{++-}$) adult mice. Restoration of *Dyrk1a* gene copy number in trisomic mice reduces the amount of Dyrk1a protein to the levels of their $Dyrk1a^{+/+}$ littermates. Immunodetection of actin was used as a loading control. The histogram shows the average relative protein level calculated from western blots performed with three independent retinal lysates. (**B**) The histogram shows the average number of active Casp9+ retinal cells in P0 mice of the four genotypes. Note that there is no difference in the number of active Casp9+ cells between Ts$Dyrk1a^{++-}$ mice and control euploid mice: $n = 4$ (euploid); $n = 3$ ($Dyrk1a^{+/-}$); $n = 4$ (Ts$Dyrk1a^{+++}$); $n = 3$ (Ts$Dyrk1a^{++-}$). (**C**) Representative retinal cross-sections from the eyes of 1-month-old $Dyrk1a^{+/+}$, Ts$Dyrk1a^{+++}$, Ts$Dyrk1a^{++-}$ and $Dyrk1a^{+/-}$ mice. Note that the INL and IPL are thicker in Ts$Dyrk1a^{+++}$ mice than in control euploid mice, but not in Ts$Dyrk1a^{++-}$ mice. Scale bar corresponds to 40 μm. (**D**) The histograms showing the average total retina thickness (left) and the thickness of the outer and inner nuclear and plexiform layers (right) in eye sections from animals of the four genotypes, like those shown in (C): $n = 10$ (euploid); $n = 6$ ($Dyrk1a^{+/-}$); $n = 6$ (Ts$Dyrk1a^{+++}$); $n = 8$ (Ts$Dyrk1a^{++-}$). The mean values were compared with the values in euploid mice. $^{**}P < 0.001$ and $^{***}P < 0.0001$.

overexpression. To confirm this hypothesis, we tested whether normalizing *Dyrk1a* gene copy number in Ts65Dn mice restored retinal function by obtaining ERGs from the progeny of Ts65Dn and $Dyrk1a^{+/-}$ crosses. Adult Ts65Dn (Ts$Dyrk1a^{+++}$) animals had increased scotopic and photopic b-wave amplitudes (Fig. 5A, B, D and F). Maximum scotopic OP amplitudes (Fig. 5C) and flicker responses (Fig. 5E) were greater in Ts$Dyrk1a^{+++}$ mice than in controls, although the differences between genotypes did not reach significance (Fig. 5F). Scotopic a-wave amplitudes in these animals were normal (Fig. 5B and F) as in the previous experiment in Ts65Dn mice (Fig. 3B and F). Remarkably, both the scotopic and photopic b-waves, maximum OP amplitudes and flicker responses reverted to normal in Ts$Dyrk1a^{++-}$ animals. As seen previously (16), the same electrical responses that increased in Ts$Dyrk1a^{+++}$ mice diminished in $Dyrk1a^{+/-}$ mice (Fig. 5A–F). Together, these results show that increased retinal activity in the Ts65Dn trisomic model is independent of the genetic background of the animals and it is caused by over-expression of Dyrk1a.

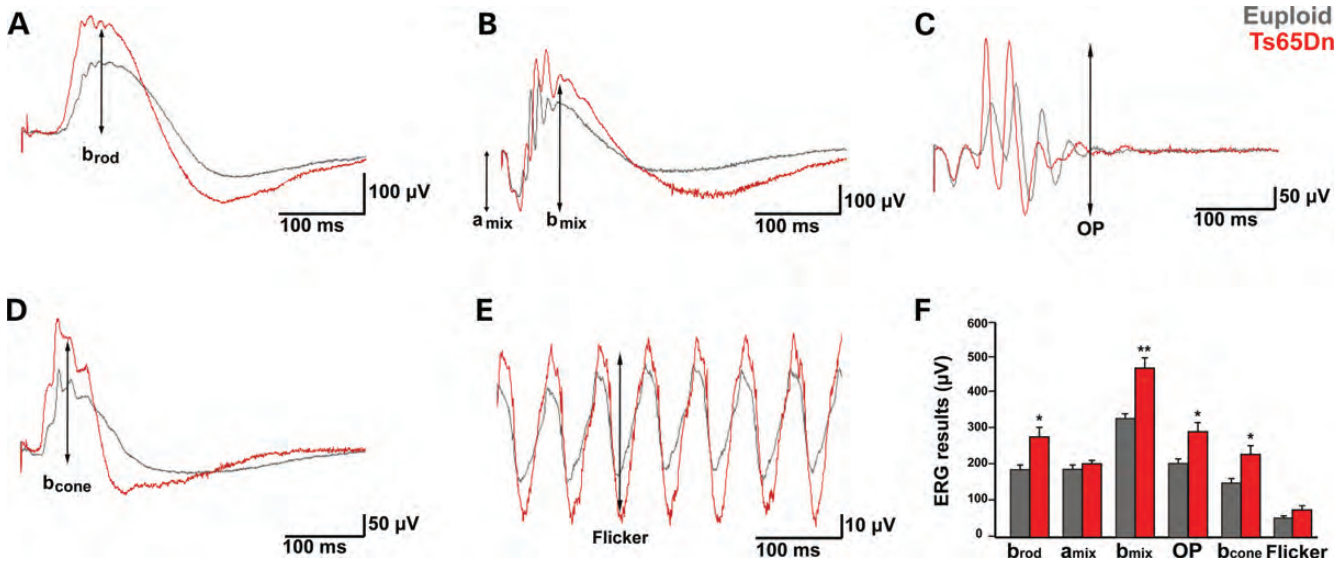

Figure 4. Increased retinal activity in Ts65Dn mice. (**A**–**E**) Representative ERG recordings obtained from one adult Ts65Dn (red traces) and one euploid (grey traces) littermate mouse. The rod- and cone-driven circuitries were tested, respectively, under scotopic (A–C) and photopic conditions (D–E). Note that the amplitudes of the scotopic b-waves (b_{rod} in A and b_{mix} in B) are larger in Ts65Dn mice than in euploid mice, whereas the a-wave amplitude (a_{mix} in B) is similar in mice of both genotypes. The maximum amplitude of OPs (OP in C) and the photopic b-wave amplitudes (b_{cone} in D) are also larger in Ts65Dn animals than in the controls. ERG responses to high-frequency flicker stimuli (E) show a trend towards larger responses in trisomic animals. Calibration groups: (A) and (B), (C) and (D), and (E). (**F**) Histogram summarizing the average ERG responses recorded in Ts65Dn and euploid mice: $n = 11$ (euploid); $n = 10$ (Ts65Dn). $^{*}P < 0.05$, $^{**}P < 0.001$.

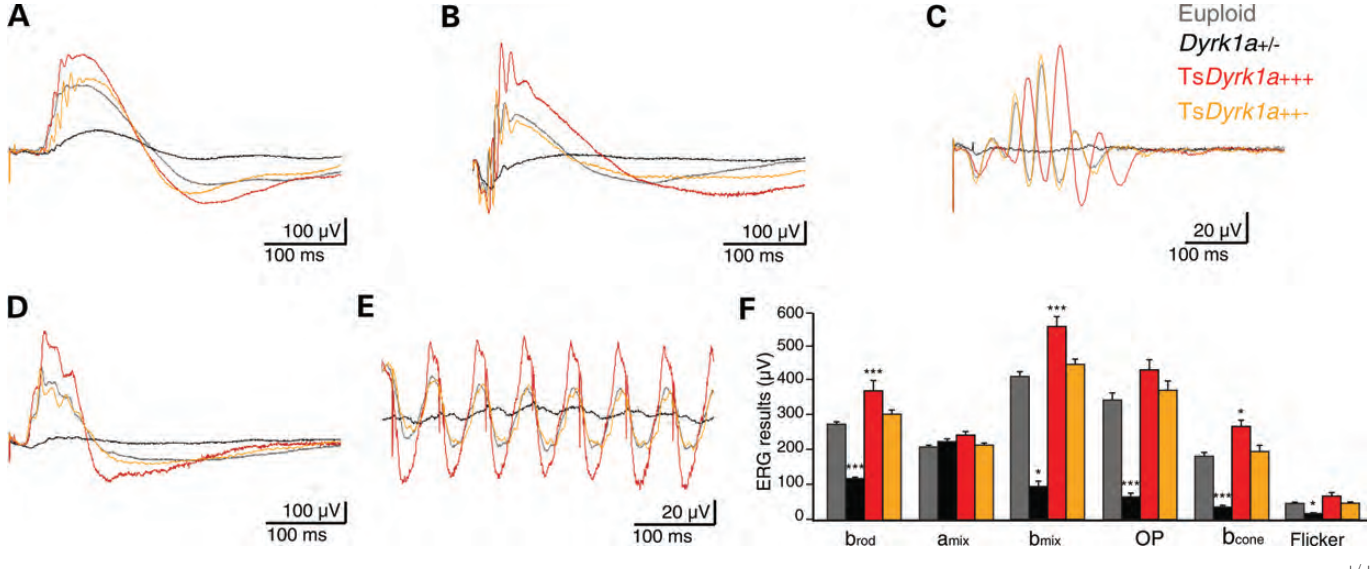

Figure 5. Reverting *Dyrk1a* gene copy number in Ts65Dn mice normalizes retinal activity. (**A**–**E**) Representative ERG recordings from a control *Dyrk1a*$^{+/+}$ (euploid) mouse (grey traces), a *Dyrk1a*$^{+/-}$ mouse (black traces), a Ts65Dn (Ts*Dyrk1a*$^{+++}$) mouse (red traces) and a Ts65Dn mouse with two functional copies of *Dyrk1a* (Ts*Dyrk1a*$^{++-}$ mouse, yellow traces). The rod- and cone-driven circuitries were tested, respectively, under scotopic (A–C) and photopic (D–E) conditions. Note that the b-wave (b_{rod} in A; b_{mix} in B; b_{cone} in D) amplitudes, maximum OP amplitudes (C) and flicker responses (E) are greater in Ts*Dyrk1a*$^{+++}$ mice than in control euploid mice (compare red and grey traces), and that such increases are restored to normal levels in animals with a normal *Dyrk1a* gene copy number (compare yellow and green traces). The b-wave and maximum OP amplitudes and flicker responses in *Dyrk1a*$^{+/-}$ mice were significantly smaller than in euploid animals (compare black and grey traces in A–E). Calibration groups: (A), (B) and (D); and (C) and (E). (**F**) Histogram summarizing the averaged ERG responses recorded in mice of each of the four genotypes: $n = 8$ (euploid); $n = 3$ (Ts*Dyrk1a*$^{+++}$); $n = 8$ (Ts*Dyrk1a*$^{++-}$); $n = 3$ (*Dyrk1a*$^{+/-}$). $^{*}P < 0.05$ and $^{***}P < 0.0001$.

DISCUSSION

In this work, we show that overexpression of Dyrk1a, due to triplication of the gene, reduces the magnitude of physiological apoptosis in the developing retina of trisomic Ts65Dn mice, which leads to an increase in retinal cellularity and activity. Importantly, a thickening of the retina similar to

that seen in the trisomic model has also been observed in individuals with DS.

Loss-of function mutations in the human (38–40), mouse (31) and *Drosophila* (41) *DYRK1A*/*minibrain* genes cause microcephaly and developmental delay. Based on the conserved role of the DYRK1A/minibrain protein kinases in brain growth, and the dose-dependent effect of *Dyrk1a* in the mouse brain (30) and retina [(16) and Fig. 2A and C and Supplementary Material, Tables S1 and S2 in this work], we propose that the alterations in retinal thickness observed in adult DS individuals (Fig. 1) are caused by the extra copy of *DYRK1A*.

This enlargement of the retina contrasts with the overall brain size reduction of DS individuals when compared with age-matched controls (23). Brain volume variations in DS and Ts65Dn mouse are region-specific and, although there are differences between trisomic humans and mice, brain regions such as the cerebellum, which are disproportionately affected in humans, are also affected in the Ts65Dn model (42). Brain volume variations in adult mBACtg*Dyrk1a* mice are also region-specific but these variations do not completely overlap with those in Ts65Dn mice (30), indicating that other genes in trisomy in addition to *Dyrk1a* contribute to the brain growth defects in the Ts65Dn model. DYRK1A has pleiotropic functions and *in vivo* evidence shows its prominent role in neuronal proliferation and neurogenesis (43). The possibility of an augmented neuron production in the retina of mBACtg-*Dyrk1a* and Ts65Dn mice has not been assessed, but the fact that hYACtg152f7 mice did not show such increase (16) and that the embryonic retinal growth in both mBACtg*Dyrk1a* and Ts65Dn models is normal (data not shown) indicate that retinogenesis in these two mutants is not significantly impaired.

In addition to the effect of DYRK1A overexpression on retinal growth and functionality reported here, *DYRK1A* trisomy may alter cerebral visual circuits, and indeed, enhanced eye-specific refinement in the dorsal lateral geniculate nuclei was detected in postnatal Ts65Dn and Ts1Rhr mice prior to sensory stimulation (44). Ts1Rhr mice have trisomy of the *DSCR* genes and two copies of the remaining genes that are trisomic in Ts65Dn mice (45). The *DSCR* gene *DSCAM* (*Down syndrome cell adhesion molecule*) regulates retinogeniculate refinement in a dose-dependent manner but *in vivo* rescue experiments indicated that other *DSCR* genes also contribute to this phenotype (44). As enhanced eye-specific refinement could be explained by an increase in retina cellularity, *DYRK1A* could be one of these genes. Finally, and since overexpression of DYRK1A modifies mouse cortical neurogenesis (46) and neuritogenesis (47), *DYRK1A* trisomy could also be at the bases of the dendritic phenotype observed in the visual cortex of children with DS (11).

Based on the phenotypes of several transgenic mice that overexpress DYRK1A (25,26,30,48,49) and on the phenotype of partial Hsa21 trisomies involving *DYRK1A* (50–52), this gene is a candidate to be responsible for the developmental brain alterations in DS. However, the effect of an extra copy of *DYRK1A* in a trisomic context has not yet been reported for any of the DS phenotypes described. We show here that *DYRK1A* is the only trisomic gene involved in the retinal phenotype of Ts65Dn mice. This, together with other recent works showing the effect of *Olig1* and *Olig2* triplication in brain embryonic neurogenesis (53) and of *Rcan1* triplication in tumour growth (54), represents compelling experimental evidence supporting the hypothesis that triplication of one gene or a reduced number of dosage-sensitive Hsa21 genes accounts for the different DS phenotypes (19).

The data presented here provide novel insights into the pathological mechanisms involved in visual information processing in DS.

MATERIALS AND METHODS

Subjects and optical imaging of the retina

All retinal imaging procedures were performed within the scope of a neurodevelopment project (see Acknowledgements) that was approved by the Ethics Committee at the University of Coimbra (Comissão de Ética da Faculdade de Medicina da Universidade de Coimbra), and following the tenets of the Declaration of Helsinki. Written informed consent was obtained from each subject and procedures of the study were fully explained.

Morphometry was performed on the neural retina using SD-OCT, Spectralis (Heidelberg Retina Angiograph, Spectralis-HRA2; Heidelberg Engineering, Heidelberg, Germany) as described elsewhere (24). SD-OCT images were obtained from an age-matched database of control subjects ($n = 16$, 30.6 ± 8.3 years) with normal ophthalmological examination and from five of the eyes from three DS patients (29.2 ± 16.6 years). All images were obtained in pupillary mydriasis, covering an area of $20^\circ \times 20^\circ$ centred in the macula. Image acquisition was performed in high-speed mode, using 25 horizontal raster scans (B-scans) and 512 A-scans (ART mode: 20 images averaged). The wavelength of the imaging system of the SD-OCT was 870 nm, the optical resolution was $\sim$7 μm in depth and 14 μm transversely, and the scan depth was 1.8 mm. Two rings were considered for analysis, ring 1 (central circle with 1 mm of diameter) and ring 2 (3 mm).

Mice

Experimental procedures were carried out according to European Union guidelines (Directive 2010/63/EU) and following protocols that were approved by the ethics committees of the PRBB (Parc de Recerca Biomèdica de Barcelona) and of the Universidad de Alcalá.

In this study, we have used P0, P30 and adult (2–6-month-old) Ts65Dn mice, mBACtg*Dyrk1a* mice and their respective wild-type littermates, as well as the mice resulting from crosses between Ts65Dn females and *Dyrk1a*$^{+/-}$ males. The generation of Ts65Dn mice, mBACtg*Dyrk1a* mice and *Dyrk1a*$^{+/-}$ mice was described elsewhere (20,30,31). These mice were maintained in their original genetic backgrounds: Ts65Dn mice by repeated backcrossing of Ts65Dn females to C57BL/6JEi X C3H/HeSnJ (B6EiC3) F1 males; mBACtg*Dyrk1a* mice by repeated backcrossing of transgenic males to C57BL6/J (Charles River Laboratories France) females; and *Dyrk1a*$^{+/-}$ mice by repeated backcrossing of *Dyrk1a*$^{+/-}$ males to C57BL/6Jx129S2/SvHsd (C57–129) F1

females (Harlan Ibérica, S.L., Barcelona, Spain). Parental Ts65Dn females and B6EiC3 males were obtained from The Jackson Laboratories (Bar Harbor, ME, USA). *Dyrk1a*$^{+/-}$ and mBACtg*Dyrk1a* mice were genotyped by PCR (30,31) and Ts65Dn mice by quantitative PCR (http://www.jax.org/cyto/quanpcr.html). Because B6EiC3 mice carry the recessive retinal degeneration 1 *Pde6b*^{rd1} (Rd) mutation, we used trisomic females that were negative for the mutation to generate experimental trisomic and control euploid mice. The *Rd* mutation was genotyped as described previously (55).

Electroretinograms

ERGs were recorded from adult (3–6-month-old) mutant and wild-type littermates by an observer blind to the experimental condition of the animal. Prior to ERG recording, mice were dark-adapted overnight, they were then anaesthetized under dim red light with an i.p. injection of a ketamine (95 mg/kg) and xylazine (5 mg/kg) solution and kept on a heating pad maintained at 37°C. The pupils of the mice were dilated by applying a topical drop of 1% tropicamide (Culircusí Tropicamida, Alcon Cusí, El Masnou, Barcelona, Spain). To optimize electrical recording, a topical drop of 2% Methocel (Ciba Vision, Hetlingen, Switzerland) was instilled into each eye immediately before situating the corneal electrode. Flash-induced ERG responses were recorded from the right eye in response to light stimuli produced with a Ganzfeld stimulator, the intensity of which was measured with a photometer (Ciba Vision) situated at the level of the eye. For each intensity of light, 4–64 consecutive stimuli were averaged, with a 10 s interval between light flashes in scotopic conditions and of up to 60 s for the highest intensity flashes. In contrast, the interval between light flashes was fixed at 1 s under photopic conditions.

The ERG signals were amplified and band-filtered between 0.3 and 1000 Hz with a Grass amplifier (CP511 AC amplifier, Grass Instruments, Quincy, MA, USA), and then the electrical signals were digitized at 20 kHz with a Power Lab data acquisition board (AD Instruments, Chalgrove, UK). Bipolar recording was performed between an electrode fixed on a corneal lens (Burian-Allen electrode, Hansen Ophthalmic Development Lab, Coralville, IA, USA) and a reference electrode located in the mouth, with a ground electrode situated on the tail. Rod-mediated responses were recorded under dark adaptation to light flashes of -2 log cd s m^{-2}, whereas mixed rod- and cone-mediated responses were recorded in response to light flashes of 0.48 log cd s m^{-2}. OPs were isolated using white flashes of 0.48 log cd s m^{-2} in a 100–10 000 Hz range of recording frequencies. Cone-mediated responses to light flashes of 1.48 log cd s m^{-2} were recorded on a rod-saturating background of 30 cd m^{-2}. Flicker responses (20 Hz) to light flashes of 1.48 log cd s m^{-2} were recorded under a rod-saturating background of 30 cd m^{-2}. The amplitudes of the a-wave and b-wave were measured off-line and the results averaged.

Western blotting

Total protein extracts from the adult retina (~80 μg) were resolved by SDS–PAGE and transferred onto a nitrocellulose membrane (Hybond-ECL, Amersham Biosciences), which was then probed as described previously (16). The antibodies used were a mouse monoclonal anti-DYRK1A (1:500; Abnova Corporation); a rabbit polyclonal anti-α-actin (1:5000; Sigma); and a goat anti-mouse IgG IRDye-800CW or a goat anti-rabbit IgG IRDye-680CW (1:5000; LI-COR ODYSSEY). Fluorescence was detected and quantified using the LI-COR Odyssey IR Imaging System V3.0 (LI-COR Biosciences, Lincoln, NE, USA).

Eye processing for histology

P0 animals were sacrificed with an overdose of isofluorane, and their heads were recovered and fixed by immersion in 4% paraformaldehyde (PFA) in 0.1 M phosphate buffer (PB, pH 7.4) for 24 h at 4°C. The heads were then cryoprotected, embedded in Tissue-Tek O.C.T. (Sakura), frozen in isopentane (Panreac) and sectioned on a cryostat. Cryosections (16 μm) were collected on Starfrost-precoated slides (Knittel Glasser) and distributed serially. P30 and adult mice (2-month-old) were deeply anaesthetized and transcardially perfused with 4% PFA in PB at RT. The eyecups were removed from these mice and post-fixed by immersion in the same fixative for 24 h at 4°C. After dehydration in an ethanol gradient and embedding in paraffin (Merck), transverse sections (5 μm) were obtained with a sliding microtome, and sections containing the optic nerve were collected on poly-L-lysine-coated slides.

Morphometry and cell numbers

Paraffin sections stained with cresyl violet acetate were used to quantify morphological parameters of the retina. The size of the retina and of each retina layer and the number of cells in the GC layer were estimated using an Olympus BX51 microscope and the CAST GRID stereological software package from Olympus as described previously (16). Only central sections were considered for the analysis, defined as transverse sections containing a complete section of the optic nerve opposite the cornea. A minimum of four animals per genotype was included in the analysis.

Apoptosis

Developmental apoptosis was evaluated in P0 mice by counting the number of active Casp3- and active Casp9-immunostained cells in cryosections of the retina. The immunohistochemical procedure followed was that described previously (16), using the avidin–biotin–peroxidase method. Sections were incubated overnight at 4°C with a rabbit monoclonal anti-active Casp3 (1:1000, BD Pharmigen) or a rabbit polyclonal anti-active Casp9 (Asp353, 1:500 Cell Signaling Technology) antibody diluted in blocking buffer [0.2% Triton-X100 and 5% (v/v) fetal bovine serum (GIBCO) in PBS]. After staining with the corresponding biotinylated secondary antibodies (1:200) from Vector Labs, the total number of apoptotic cells in the retina was calculated by counting Casp3 and Casp9 immunopositive cells in one complete series from at least three animals per genotype.

Statistical analysis

To compare the thickness between control and DS retinas, the Mann–Whitney *U* test with Bonferroni correction for multiple comparisons was applied using the SPSS (version 18) software package. These data are presented as the mean ± standard deviation. In the rest of experiments, the significance of the differences between the groups was evaluated by analysis of variance followed by a two-tailed Student's *t*-test. These data are presented as the mean ± standard error of the mean. In all the experiments, the differences are considered to be significant at *P*-values <0.05.

SUPPLEMENTARY MATERIAL

Supplementary Material is available at *HMG* online.

ACKNOWLEDGEMENTS

We thank all the subjects and their families for participating in the human study reported here. The authors wish to express their gratitude to Aldina Reis and Laura Ramírez for their technical assistance, to Sonia Najas and Susana García for their help in preparing and genotyping the mouse tissue, to Mark Sefton for English editorial work and to the personnel of the PRBB animal facility for taking care of the mice.

Conflict of Interest statement. None declared.

FUNDING

This work was supported by the Spanish Ministry of Economy and Competitiveness (grant numbers SAF-2007-60940 and SAF-2010-17004 to M.L.A., and SAF-2010-21879 to P.dlV.), by the Generalitat de Catalunya (grant number 2009SGR1464) and by the Portuguese Foundation for Science and Technology (grant numbers PIC/IC/82986/2007 and Compete/PTDC/SAU/ORG_118380). A.L. was supported by an FI grant (AGAUR, Generalitat de Cataluya) and M.-J.B. by the CIBERER.

REFERENCES

1. Pueschel, S.M. (1990) Clinical aspects of Down syndrome from infancy to adulthood. *Am. J. Med. Genet. Suppl.*, **7**, 52–56.
2. Antonarakis, S.E., Lyle, R., Dermitzakis, E.T., Reymond, A. and Deutsch, S. (2004) Chromosome 21 and down syndrome: from genomics to pathophysiology. *Nat. Rev. Genet.*, **5**, 725–738.
3. Catalano, R.A. (1990) Down syndrome. *Surv. Ophthalmol.*, **34**, 385–398.
4. Creavin, A.L. and Brown, R.D. (2009) Ophthalmic abnormalities in children with Down syndrome. *J. Pediatr. Ophthalmol. Strabismus*, **46**, 76–82.
5. da Cunha, R.P. and Moreira, J.B. (1996) Ocular findings in Down's syndrome. *Am. J. Ophthalmol.*, **122**, 236–244.
6. Courage, M.L., Adams, R.J., Reyno, S. and Kwa, P.G. (1994) Visual acuity in infants and children with Down syndrome. *Dev. Med. Child. Neurol.*, **36**, 586–593.
7. Courage, M.L., Adams, R.J. and Hall, E.J. (1997) Contrast sensitivity in infants and children with Down syndrome. *Vision. Res.*, **37**, 1545–1555.
8. John, F.M., Bromham, N.R., Woodhouse, J.M. and Candy, T.R. (2004) Spatial vision deficits in infants and children with Down syndrome. *Invest. Ophthalmol. Vis. Sci.*, **45**, 1566–1572.
9. Suttle, C.M. and Lloyd, R. (2005) Chromatic and achromatic transient VEPs in adults with Down syndrome. *Ophthalmic Physiol. Opt.*, **25**, 501–513.
10. Chen, Y.J. and Fang, P.C. (2005) Sensory evoked potentials in infants with Down syndrome. *Acta Paediatr.*, **94**, 1615–1618.
11. Becker, L.E., Armstrong, D.L. and Chan, F. (1986) Dendritic atrophy in children with Down's syndrome. *Ann. Neurol.*, **20**, 520–526.
12. Evenhuis, H.M., Sjoukes, L., Koot, H.M. and Kooijman, A.C. (2009) Does visual impairment lead to additional disability in adults with intellectual disabilities? *J. Intellect. Disabil. Res.*, **53**, 19–28.
13. Masland, R.H. (2012) The neuronal organization of the retina. *Neuron*, **76**, 266–280.
14. Donovan, S.L. and Dyer, M.A. (2005) Regulation of proliferation during central nervous system development. *Semin. Cell Dev. Biol.*, **16**, 407–421.
15. Stewart, L., Potok, M.A., Camper, S.A. and Stifani, S. (2005) Runx1 expression defines a subpopulation of displaced amacrine cells in the developing mouse retina. *J. Neurochem.*, **94**, 1739–1745.
16. Laguna, A., Aranda, S., Barallobre, M.J., Barhoum, R., Fernandez, E., Fotaki, V., Delabar, J.M., de la Luna, S., de la Villa, P. and Arbones, M.L. (2008) The protein kinase DYRK1A regulates caspase-9-mediated apoptosis during retina development. *Dev. Cell*, **15**, 841–853.
17. Fuerst, P.G., Bruce, F., Tian, M., Wei, W., Elstrott, J., Feller, M.B., Erskine, L., Singer, J.H. and Burgess, R.W. (2009) DSCAM and DSCAML1 function in self-avoidance in multiple cell types in the developing mouse retina. *Neuron*, **64**, 484–497.
18. Hafler, B.P., Surzenko, N., Beier, K.T., Punzo, C., Trimarchi, J.M., Kong, J.H. and Cepko, C.L. (2012) Transcription factor Olig2 defines subpopulations of retinal progenitor cells biased toward specific cell fates. *Proc. Natl Acad. Sci. USA*, **109**, 7882–7887.
19. Haydar, T.F. and Reeves, R.H. (2012) Trisomy 21 and early brain development. *Trends Neurosci.*, **35**, 81–91.
20. Davisson, M.T., Schmidt, C., Reeves, R.H., Irving, N.G., Akeson, E.C., Harris, B.S. and Bronson, R.T. (1993) Segmental trisomy as a mouse model for Down syndrome. *Prog. Clin. Biol. Res.*, **384**, 117–133.
21. Scott-McKean, J.J., Chang, B., Hurd, R.E., Nusinowitz, S., Schmidt, C., Davisson, M.T. and Costa, A.C. (2010) The mouse model of Down syndrome Ts65Dn presents visual deficits as assessed by pattern visual evoked potentials. *Invest. Ophthalmol. Vis. Sci.*, **51**, 3300–3308.
22. Guimera, J., Casas, C., Pucharcos, C., Solans, A., Domenech, A., Planas, A.M., Ashley, J., Lovett, M., Estivill, X. and Pritchard, M.A. (1996) A human homologue of *Drosophila* minibrain (MNB) is expressed in the neuronal regions affected in Down syndrome and maps to the critical region. *Hum. Mol. Genet.*, **5**, 1305–1310.
23. Pinter, J.D., Eliez, S., Schmitt, J.E., Capone, G.T. and Reiss, A.L. (2001) Neuroanatomy of Down's syndrome: a high-resolution MRI study. *Am. J. Psychiatry*, **158**, 1659–1665.
24. Sabates, F.N., Vincent, R.D., Koulen, P., Sabates, N.R. and Gallimore, G. (2011) Normative data set identifying properties of the macula across age groups: integration of visual function and retinal structure with microperimetry and spectral-domain optical coherence tomography. *Retina*, **31**, 1294–1302.
25. Smith, D.J., Stevens, M.E., Sudanagunta, S.P., Bronson, R.T., Makhinson, M., Watabe, A.M., O'Dell, T.J., Fung, J., Weier, H.U., Cheng, J.F. *et al.* (1997) Functional screening of 2 Mb of human chromosome 21q22.2 in transgenic mice implicates minibrain in learning defects associated with Down syndrome. *Nat. Genet.*, **16**, 28–36.
26. Branchi, I., Bichler, Z., Minghetti, L., Delabar, J.M., Malchiodi-Albedi, F., Gonzalez, M.C., Chettouh, Z., Nicolini, A., Chabert, C., Smith, D.J. *et al.* (2004) Transgenic mouse in vivo library of human Down syndrome critical region 1: association between DYRK1A overexpression, brain development abnormalities, and cell cycle protein alteration. *J. Neuropathol. Exp. Neurol.*, **63**, 429–440.
27. Riedl, S.J. and Salvesen, G.S. (2007) The apoptosome: signalling platform of cell death. *Nat. Rev. Mol. Cell Biol.*, **8**, 405–413.
28. Isenmann, S., Kretz, A. and Cellerino, A. (2003) Molecular determinants of retinal ganglion cell development, survival, and regeneration. *Prog. Retin. Eye Res.*, **22**, 483–543.
29. Guerin, M.B., McKernan, D.P., O'Brien, C.J. and Cotter, T.G. (2006) Retinal ganglion cells: dying to survive. *Int. J. Dev. Biol.*, **50**, 665–674.
30. Guedj, F., Pereira, P.L., Najas, S., Barallobre, M.J., Chabert, C., Souchet, B., Sebrie, C., Verney, C., Herault, Y., Arbones, M. *et al.* (2012) DYRK1A: a master regulatory protein controlling brain growth. *Neurobiol. Dis.*, **46**, 190–203.

31. Fotaki, V., Dierssen, M., Alcantara, S., Martinez, S., Marti, E., Casas, C., Visa, J., Soriano, E., Estivill, X. and Arbones, M.L. (2002) Dyrk1A haploinsufficiency affects viability and causes developmental delay and abnormal brain morphology in mice. *Mol. Cell Biol.*, **22**, 6636–6647.
32. Young, R.W. (1984) Cell death during differentiation of the retina in the mouse. *J. Comp. Neurol.*, **229**, 362–373.
33. Cellerino, A., Bahr, M. and Isenmann, S. (2000) Apoptosis in the developing visual system. *Cell Tissue Res.*, **301**, 53–69.
34. Farah, M.H. and Easter, S.S. Jr (2005) Cell birth and death in the mouse retinal ganglion cell layer. *J. Comp. Neurol.*, **489**, 120–134.
35. Bramblett, D.E., Pennesi, M.E., Wu, S.M. and Tsai, M.J. (2004) The transcription factor Bhlhb4 is required for rod bipolar cell maturation. *Neuron*, **43**, 779–793.
36. Brzezinski, J.A. IV, Brown, N.L., Tanikawa, A., Bush, R.A., Sieving, P.A., Vitaterna, M.H., Takahashi, J.S. and Glaser, T. (2005) Loss of circadian photoentrainment and abnormal retinal electrophysiology in Math5 mutant mice. *Invest. Ophthalmol. Vis. Sci.*, **46**, 2540–2551.
37. Pugh, E.N. Jr, Falsini, B. and Lyubarsky, A.L. (1998) In: Thistle, A.B. and Williams, T.P. (eds), *Photostasis and Related Topics*. Plenum, New York, NY, pp. 93–128.
38. Courcet, J.B., Faivre, L., Malzac, P., Masurel-Paulet, A., Lopez, E., Callier, P., Lambert, L., Lemesle, M., Thevenon, J., Gigot, N. *et al.* (2012) The DYRK1A gene is a cause of syndromic intellectual disability with severe microcephaly and epilepsy. *J. Med. Genet.*, **49**, 731–736.
39. van Bon, B.W., Hoischen, A., Hehir-Kwa, J., de Brouwer, A.P., Ruivenkamp, C., Gijsbers, A.C., Marcelis, C.L., de Leeuw, N., Veltman, J.A., Brunner, H.G. *et al.* (2011) Intragenic deletion in DYRK1A leads to mental retardation and primary microcephaly. *Clin. Genet.*, **79**, 296–299.
40. Moller, R.S., Kubart, S., Hoeltzenbein, M., Heye, B., Vogel, I., Hansen, C.P., Menzel, C., Ullmann, R., Tommerup, N., Ropers, H.H. *et al.* (2008) Truncation of the Down syndrome candidate gene DYRK1A in two unrelated patients with microcephaly. *Am. J. Hum. Genet.*, **82**, 1165–1170.
41. Tejedor, F., Zhu, X.R., Kaltenbach, E., Ackermann, A., Baumann, A., Canal, I., Heisenberg, M., Fischbach, K.F. and Pongs, O. (1995) minibrain: a new protein kinase family involved in postembryonic neurogenesis in *Drosophila*. *Neuron*, **14**, 287–301.
42. Baxter, L.L., Moran, T.H., Richtsmeier, J.T., Troncoso, J. and Reeves, R.H. (2000) Discovery and genetic localization of Down syndrome cerebellar phenotypes using the Ts65Dn mouse. *Hum. Mol. Genet.*, **9**, 195–202.
43. Tejedor, F.J. and Hammerle, B. (2011) MNB/DYRK1A as a multiple regulator of neuronal development. *FEBS J.*, **278**, 223–235.
44. Blank, M., Fuerst, P.G., Stevens, B., Nouri, N., Kirkby, L., Warrier, D., Barres, B.A., Feller, M.B., Huberman, A.D., Burgess, R.W. *et al.* (2011) The Down syndrome critical region regulates retinogeniculate refinement. *J. Neurosci.*, **31**, 5764–5776.
45. Olson, L.E., Roper, R.J., Sengstaken, C.L., Peterson, E.A., Aquino, V., Galdzicki, Z., Siarey, R., Pletnikov, M., Moran, T.H. and Reeves, R.H. (2007) Trisomy for the Down syndrome 'critical region' is necessary but not sufficient for brain phenotypes of trisomic mice. *Hum. Mol. Genet.*, **16**, 774–782.
46. Yabut, O., Domogauer, J. and D'Arcangelo, G. (2010) Dyrk1A overexpression inhibits proliferation and induces premature neuronal differentiation of neural progenitor cells. *J. Neurosci.*, **30**, 4004–4014.
47. Martinez de Lagran, M., Benavides-Piccione, R., Ballesteros-Yanez, I., Calvo, M., Morales, M., Fillat, C., Defelipe, J., Ramakers, G.J. and Dierssen, M. (2012) Dyrk1A influences neuronal morphogenesis through regulation of cytoskeletal dynamics in mammalian cortical neurons. *Cereb. Cortex*, **22**, 2867–2877.
48. Altafaj, X., Dierssen, M., Baamonde, C., Marti, E., Visa, J., Guimera, J., Oset, M., Gonzalez, J.R., Florez, J., Fillat, C. *et al.* (2001) Neurodevelopmental delay, motor abnormalities and cognitive deficits in transgenic mice overexpressing Dyrk1A (minibrain), a murine model of Down's syndrome. *Hum. Mol. Genet.*, **10**, 1915–1923.
49. Ahn, K.J., Jeong, H.K., Choi, H.S., Ryoo, S.R., Kim, Y.J., Goo, J.S., Choi, S.Y., Han, J.S., Ha, I. and Song, W.J. (2006) DYRK1A BAC transgenic mice show altered synaptic plasticity with learning and memory defects. *Neurobiol. Dis.*, **22**, 463–472.
50. Delabar, J.M., Theophile, D., Rahmani, Z., Chettouh, Z., Blouin, J.L., Prieur, M., Noel, B. and Sinet, P.M. (1993) Molecular mapping of twenty-four features of Down syndrome on chromosome 21. *Eur. J. Hum. Genet.*, **1**, 114–124.
51. Korenberg, J.R., Aaltonen, J., Brahe, C., Cabin, D., Creau, N., Delabar, J.M., Doering, J., Gardiner, K., Hubert, R.S., Ives, J. *et al.* (1997) Report and abstracts of the Sixth International Workshop on Human Chromosome 21 Mapping 1996. Cold Spring Harbor, New York, USA. May 6–8,1996. *Cytogenet. Cell Genet.*, **79**, 21–52.
52. Ronan, A., Fagan, K., Christie, L., Conroy, J., Nowak, N.J. and Turner, G. (2007) Familial 4.3 Mb duplication of 21q22 sheds new light on the Down syndrome critical region. *J. Med. Genet.*, **44**, 448–451.
53. Chakrabarti, L., Best, T.K., Cramer, N.P., Carney, R.S., Isaac, J.T., Galdzicki, Z. and Haydar, T.F. (2010) Olig1 and Olig2 triplication causes developmental brain defects in Down syndrome. *Nat. Neurosci.*, **13**, 927–934.
54. Baek, K.H., Zaslavsky, A., Lynch, R.C., Britt, C., Okada, Y., Siarey, R.J., Lensch, M.W., Park, I.H., Yoon, S.S., Minami, T. *et al.* (2009) Down's syndrome suppression of tumour growth and the role of the calcineurin inhibitor DSCR1. *Nature*, **459**, 1126–1130.
55. Pittler, S.J. and Baehr, W. (1991) Identification of a nonsense mutation in the rod photoreceptor cGMP phosphodiesterase beta-subunit gene of the rd mouse. *Proc. Natl Acad. Sci. USA*, **88**, 8322–8326.